JPET Fast Forward. Published on September 14, 2017 as DOI: 10.1124/jpet.117.244020
This article has not been copyedited and formatted. The final version may differ from this version.

A novel bibenzyl compound, 20C, protected mice from MPTP/p toxicity by regulating α-synuclein related inflammatory response

Qiu-Shuang Zhang, Yang Heng, Ying Chen, Piao Luo, Lu Wen, Zhao Zhang, Yu-He Yuan, Nai-Hong Chen

State Key Laboratory of Bioactive Substances and Functions of Natural Medicines, Institute of Materia Medica & Neuroscience Center, Chinese Academy of Medical Sciences and Peking Union Medical College, Beijing 100050, China (Qiu-Shuang Zhang, Yang Heng, Ying Chen, Lu Wen, Zhao Zhang, Yu-He Yuan, Nai-Hong Chen); College of Pharmacy, Hunan University of Chinese Medicine, Changsha, Hunan 410208, China (Piao Luo, Nai-Hong Chen)

JPET Fast Forward. Published on September 14, 2017 as DOI: 10.1124/jpet.117.244020
This article has not been copyedited and formatted. The final version may differ from this version.

Running title: 20C protects against MPTP/p toxicity by targeting α-synuclein

Corresponding author:

Yu-He Yuan

Department of Pharmacology, Institute of Materia Medica, Chinese Academy of Medical Sciences and Peking Union Medical College

Xiannongtan Street, Xicheng District, Beijing 100050, P.R. China,

Tel: +86 10 63165182; Fax: +86 10 63165177

E-mail: yuanyuhe@imm.ac.cn

Nai-Hong Chen

Department of Pharmacology, Institute of Materia Medica, Chinese Academy of Medical Sciences and Peking Union Medical College

Xiannongtan Street, Xicheng District, Beijing 100050, P.R. China

Tel: +86 10 63165177; Fax: +86 10 63165177

E-mail: chennh@imm.ac.cn

Number of pages: 32

Number of figures: 6

Number of references: 35

Abstract word count: 127

Introduction word count: 397

Discussion word count: 1360

Abbreviations

BBB: blood-brain barrier; Ctrl: control; DA: dopamine; DMSO: dimethyl sulfoxide;

DOPAC: dihydroxyphenylacetic acid; GFAP: glial fibrillary acidic protein; GSDMD: Gasdermin D; HPLC: high performance liquid column; HVA: homovanillic acid; i.p.: intraperitoneal; IBA-1: ionized calcium binding adapter molecule-1; IL-1β: interleukin-1β; IL-6: interleukin-6; INF-γ: interferon-γ; LBs: Lewy bodies; MAO-B: monoamine oxidase type B; MPP^+: 1-methyl-4-phenyl-pyridinium ion; MPTP: 1-methyl-4-phenyl-1, 2, 3, 6-tetrahydropyridine; MPTP/p: MPTP/probenecid; NF-κB: nuclear factor-kappa B; NLRP3: NOD-like receptor protein 3; PD: Parkinson's disease; rpm: revolutions per minute; s.c.: subcutaneous injection; SEM: standard error of mean; SN: substantia nigra; SNpc: substantia nigra pars compact; TEM: transmission electron microscope; TH: tyrosine hydroxylase; TLR4: toll-like receptor 4.

Recommended section assignment: Neuropharmacology

JPET Fast Forward. Published on September 14, 2017 as DOI: 10.1124/jpet.117.244020
This article has not been copyedited and formatted. The final version may differ from this version.

Abstract

The novel bibenzyl compound 20C plays a neuroprotective role *in vitro*, but its effects *in vivo* have not been elucidated. In this study, we estimated the efficacy of 20C *in vivo* using a 1-methyl-4-phenyl-1, 2, 3, 6-tetrahydropyridine/probenecid (MPTP/p) mouse model from behavior, dopamine and neuron, and then the possible mechanisms for these effects were further investigated. The experimental results showed that 20C improved behavioral deficits, attenuated dopamine depletion, reduced dopaminergic neuron loss, protected blood brain barrier structure, ameliorated α-synuclein dysfunction, suppressed glial activation, and regulated both NF-κB signaling and the NLRP3 inflammasome pathway. Our results indicated that 20C may prevent neurodegeneration in the MPTP/p mouse model by targeting α-synuclein and regulating α-synuclein related inflammatory responses, including BBB damage, glial activation, NF-κB signaling, and the NLRP3 inflammasome pathway.

Introduction

Parkinson's disease (PD) is well known for motor disorders such as resting tremor, bradykinesia, muscle rigidity, and postural instability, and affects 1% of the population over 60 years old (Connolly and Lang, 2014). Typical characteristics of PD include progressive loss of dopaminergic cells in the substantia nigra pars compacta (SNpc), dopamine (DA) depletion in the striatum and formation of Lewy bodies (LBs) (Connolly and Lang, 2014). The current therapy for PD relies on DA supplementation from its precursor, L-dopa, which can quickly improve behavioral symptoms, but long time treatment with L-dopa may induce considerable adverse effects (Connolly and Lang, 2014). Therefore, it is necessary to develop new efficient candidates based on PD pathogenesis. The exact etiology for PD remains unknown, and neurotoxin-based experimental models of PD have been widely used to mimic the clinical parkinsonian features. To some extent, these models conform to a hypothesis of pathogenesis that involves α-synuclein dysfunction, inflammation, and oxidative stress(Zhang et al., 2017a) (Dauer and Przedborski, 2003). Among these models, the 1-methyl-4-phenyl-1, 2, 3, 6-tetrahydropyridine (MPTP)-induced animal model is widely used in the study of PD. MPTP can cross the blood brain barrier (BBB) and be metabolized into its toxic form 1-methyl-4-phenylpyridinium iron (MPP^+) by monoamine oxidase B (MAO-B) in the glia, and then MPP^+ can be transferred to dopaminergic neurons via dopamine transporters to induce cell death (Dauer and Przedborski, 2003). The chronic MPTP/probenecid (MPTP/p) model is more popular than others to mimic the neurodegenerative process of PD. In this model, probenecid is applied to enhance the

toxicity of MPTP by suppressing its clearance (Bove and Perier, 2012). The specific MAO-B inhibitor, selegiline, is a reliable reference for efficacy evaluation in this model. The traditional herbal medicine, *Gastrodia elata* (Tianma), has been used for centuries to treat headache, dizziness, epilepsy, rheumatism, neuralgia, paralysis, and other neuralgic disorders (Ojemann et al., 2006). Moreover, Tianma (*Gastrodia elata*) Gouteng Yin has been commonly prescribed in China to treat parkinsonian symptoms including tremor and paralysis (Liu et al., 2015). 20C is a novel bibenzyl compound derived from *Gastrodia elata*, and its neuroprotective effect *in vitro* has been described; it has been found to promote anti-apoptosis and oxidation resistance, reduce α-synuclein accumulation, and inhibit endoplasmic reticulum stress (Huang et al., 2016; Mou et al., 2016; Zhang et al., 2017c). In this study, we investigated its protective effect and associated mechanism *in vivo* using the MPTP/p mouse model.

Materials and methods

Reagents and Animals

The compound 20C (Figure 1A) was provided by the Department of Chemosynthesis, Institute of Materia Medica, Chinese Academy of Medical Sciences and Peking Union Medical College (Beijing, China). Selegiline hydrochloride (Orion Co., Espoo, Finland) was purchased from Beijing hospital. MPTP hydrochloride and probenecid were obtained from Sigma Corporation (Sigma Co., St. Louis, MO). Male C57BL/6 mice (8 weeks, 22–25 g, Charles River Co., Beijing, China) were used into experiments. All mice were housed on a cycle of 12 h light/dark, in a temperature of 22 ± 1 ℃, with free access to food and water. All experiments on animals were approved by the Animal

Care Committee of the Chinese Academy of Medical Sciences, according to the principles established for the care and use of laboratory animals by the National Institutes of Health.

Experimental procedures

After one week of adaptation, all animals were randomly divided into six groups (Figure 1B): the control group (equivoluminal water), the model group (equivoluminal water), the 20C groups (25, 50, 100 mg/kg), and the selegiline group (3 mg/kg). Then, they were trained in the pole test. The chronic mouse model was established as follows (Figure 1C). One hour after intraperitoneal injection of probenecid (250 mg/kg b.w., dissolved in 0.1 M NaOH-Tris-HCl, PH = 7.4), the mice were subcutaneously injected with MPTP-HCl (25 mg/kg, dissolved in 0.9% saline, s.c.). This process of MPTP/p injection was conduct every 4 days and a total of 10 doses were administered. 20C, selegiline or equivoluminal water were administered three days before starting this MPTP/p scheme, and the administration continued for fifty-three days. After completing the MPTP/p administration protocol, the pole test was implemented to assess the behavioral performance of mice. Ten days after the last injection, mice were sacrificed for further study.

Behavioral testing

Behavioral performance was evaluated with the pole test as described in our previous work (Heng et al., 2016). The test's objective is to measure the time required for the mice to climb down from the top of the pole. After adaptation, the mice were pre-trained in the pole apparatus for three sessions to make sure that all animals for experiments

JPET Fast Forward. Published on September 14, 2017 as DOI: 10.1124/jpet.117.244020
This article has not been copyedited and formatted. The final version may differ from this version.

would climb down as soon as they were put on the ball. During testing, the time required to climb down was recorded.

Tissue preparation

For the biochemical analysis, mice were deeply anesthetized with chloral hydrate (400 mg/kg, i.p.), and brain tissues were rapidly isolated and stored at -80 ℃. For the histological analysis after anesthesia, mice were perfused intracardially with 0.1 M phosphate-buffered saline (PBS) and 4% paraformaldehyde. Then, the mouse brains were collected and preserved in 4% paraformaldehyde. Before detection, the brain samples were dehydrated with graded sucrose (10%, 20%, and 30%), and then coronal sections (20 μm), containing the striatum region or the substantia nigra pars compacta (SNpc) region, were dissected on a cryostat (CM3050S, Leica, Germany). Finally, these sections were laid on coated slides for detection.

High performance liquid chromatography (HPLC)

Tissues of the striatum were 10-fold diluted (w/v) with ice-cold solution A, which contained 0.6 M $HClO_4$ and 375 ng/ml isoprenaline, homogenized, and centrifuged at 20,000 g at 4 ℃ for 20 min. The supernatant was collected and mixed with half-volume solution B — containing 20 mM potassium citrate, 300 mM K_2HPO_4, and 2 mM EDTA-2Na — and centrifuged again, filtered, and injected into the HPLC system (Waters e2695; Waters, Milford, MA) equipped with a C18 column (4.6 mm, 150 mm; Atlantis T3; Waters) and an electrochemical detector (Waters 2465; Waters). The mobile phase (100 mM sodium acetate anhydrous, 85 mM citric acid, 0.5 mM 1-octanesulfonic acid sodium, 0.2 mM EDTA-2Na, 15% methanol, pH = 3.68) was pumped at a rate of 1

ml/min. The detecting potential was set at 760 mV versus Ag/AgCl and the assay sensitivity was set at a scale of 50 nA.

Western blot analysis

After the striatum tissue disrupted and centrifuged, the supernatant was collected, measured using a BCA kit, and denatured in loading buffer. Samples of equal protein content were separated by 15% polyacrylamide gel electrophoresis and transferred to polyvinylidene difluoride membranes (Millipore, Milford, MA). After blocked with 3% bovines serum albumin (BSA) (Sigma-Aldrich), these membranes were incubated with primary antibodies, such as anti-beta-actin (1:5000, Sigma), anti-tyrosine hydroxylase (TH) (1:500, Santa Cruz, Santa Cruz, CA), anti-α-synuclein (C20) (1:500, Santa Cruz), anti-5G4 (1:1000, Millipore), anti-nitrated Tyr125/Tyr133 α-synuclein (1:1000, Thermo, Waltham, MA), anti-phosphorylated α-synuclein (1:1000, Abcam, Cambridge, MA), anti-TLR4 (1: 250, Santa Cruz), anti-NF-κB (1:500, Santa Cruz), anti-NLRP3 (1:1000, Abcam), anti-caspase-1 (1:1000, Abcam), anti-interleukin-1-β (IL-1β) (1: 250, Santa Cruz), and anti-Gasdermin D (GSDMD) (1:1000, Sigma). Following washing, membranes were incubated with horseradish peroxidase-conjugated secondary antibody (1:5000, KPL, Gaithersburg, MD) for 2 h. The blots were detected by enhanced chemiluminescence (ECL) plus the Lmax detection system (Molecular Devices, Sunnyvale, CA) and quantified with the image analysis software (Quantity One, Toyobo, Japan).

Electron microscopic analysis

The anesthetized mice were perfused and fixed with 4% paraformaldehyde, and cubical

JPET Fast Forward. Published on September 14, 2017 as DOI: 10.1124/jpet.117.244020
This article has not been copyedited and formatted. The final version may differ from this version.

sections (1 mm^3) of the SNpc region were dissected and fixed in 2.5% glutaraldehyde for 2 h. Following washing, these samples were dehydrated in graded alcohol solution and embedded in Epon resin. Then, the regions of interest were cut into ultrathin sections, which were then doubly stained with uranyl acetate and lead citrate. Finally, the ultrastructure of the SNpc region was observed under transmission electron microscopy (TEM) (H-7650, Hitachi, Tokyo, Japan).

Immunohistochemistry and immunofluorescence

The brain slides were boiled in 0.01 M citrate buffer solution for antigen retrieval and incubated with 1% TritonX-100 to increase antibody penetration. Then, hydrogen peroxide (3%) was used to eliminate endogenous peroxidase activity. After blocked with 5% BSA, these sections were incubated with anti-TH (1:100, Santa Cruz), anti-glial fibrillary acidic protein (GFAP) (1:500, Dako, Glostrup, Denmark), or anti-ionized calcium binding adapter molecule-1 (IBA-1) (1:100, Wako, Osaka, Japan) overnight, anti-5G4 (1:200, Millipore), anti-nitrated Tyr125/Tyr133 α-synuclein (1:200, Thermo), anti-caspase-1 p10 (1:50, Santa Cruz), anti-IL-1β (1: 50, Santa Cruz), anti-8-hydroxyguanosine (1:100, Abcam), and anti-GSDMD (1:100, Sigma). Following washing, sections were incubated with horseradish peroxidase-conjugated secondary antibody (1:200, KPL) or Alexa Fluor conjugated secondary antibody (1:500, Invitrogen, Camarillo, CA). For immunohistochemistry, sections were detected with 3,3-diaminobenzidine (DAB) and captured by Olympus BA51 photomicroscope (Tokyo, Japan). For immunofluorescence, images were acquired with a fluorescence microscope (Nikon, Tokyo, Japan) or a laser scanning confocal microscope (Leica TCS

SP2, Solms, Germany). At last, Image Pro Plus 6.0 software (Media Cybernetics) was used for cell counting at 100× magnification.

Statistical analysis

Experimental data were statistically analyzed by one-way analysis of variance (ANOVA) followed by Duncan's test. All values were displayed as mean ± SEM, and a *p*-value of < 0.05 was considered to be statistically significant.

Results

Body weight, behavior assessment, and neurotransmitter

Body weight was not significantly affected by MPTP/p treatment or 20C administration (Figure 1D). The behavioral assessment with the pole test showed that MPTP/p treated mice took longer to complete the test ($p < 0.001$), and 20C (100 mg/kg, $p < 0.05$) or selegiline ($p < 0.001$) had an improving effect (Figure 1E).

Protective effect of 20C on the nigrostriatal dopaminergic system

Dopamine (DA) in the striatum was analyzed with HPLC (Figure 2A, 2B, 2C). MPTP/p caused a marked reduction of DA, while 20C (50, 100 mg/kg, $p < 0.05$) and selegiline ($p < 0.001$) significantly increased DA content. Moreover, DA turnover occurred in the MPTP/p treated mice, that is, the value of dihydroxyphenylacetic acid (DOPAC)/DA ($p < 0.001$) and homovanillic acid (HVA)/DA ($p < 0.001$) increased significantly after MPTP/p treatment. 20C (50 mg/kg, $p < 0.01$ for DOPAC/DA, $p < 0.05$ for HVA/DA), 20C (100 mg/kg, $p < 0.05$) and selegiline ($p < 0.01$) had an improving effect. The rate-limiting enzyme in DA synthesis, TH, is highly expressed in dopaminergic neurons, so TH^+ cells are considered to represent dopaminergic neurons. Immunohistochemical staining and Western blot bands showed that the dopaminergic cells in the SNpc and the terminals in the striatum were markedly lost. 20C and selegiline had a protective effect on both dopaminergic cells and terminals (Figure 2D, 2E, 2F, 2G, and 2H).

Protective effect of 20C on the ultrastructure of the SNpc region

The ultrastructure changes in the SNpc region were further studied with TEM (Figure 2I, 2J, and 2K). As shown in the images, the normal neuron has a low electron density

and a round smooth contour, and organelle structure is relatively integrated. After MPTP/p treatment, the neuron became irregular, out of shape and obtained darker electron density, and the organelles were swollen and incomplete. 20C and selegiline ameliorated MPTP/p-induced neuronal damage (Figure 2I, 2J). Moreover, the BBB in the SNpc region was severely injured by MPTP/p, and 20C and selegiline could alleviate the injury (Figure 2K).

Protective effect of 20C on MPTP-induced α-synuclein abnormality

In this study, we detected a significant increase of different α-synuclein forms by MPTP/p treatment (Figure 3A, 3B, 3C, and 3D), such as the monomeric α-synuclein (C20) ($p < 0.01$), disease-related aggregate (5G4) ($p < 0.05$), nitrated α-synuclein (N-α-syn) ($p < 0.01$), and phosphorylated α-synuclein (P-α-syn) ($p < 0.01$). Regarding increased monomeric α-synuclein (C20), 20C (50, 100 mg/kg, $p < 0.01$) and selegiline ($p < 0.01$) had a significant suppressive effect; for abnormal α-synuclein aggregate (5G4), 20C (25, 50, 100 mg/kg, $p < 0.05$) and selegiline ($p < 0.05$) had a significant relieving effect; and for nitrated α-synuclein (n-α-syn), 20C (100 mg/kg, $p < 0.05$) and selegiline ($p < 0.01$) had a significant ameliorating effect. However, for phosphorylated α-synuclein (p-α-syn), there was no evident reduction in the 20C groups and the selegiline group. The immunohistochemical staining (Figure 3E, 3F) for abnormal α-synuclein aggregate (5G4) and nitrated α-synuclein (n-α-syn) showed the same trends with the Western blot analysis.

Suppression of 20C on MPTP-induced activation of astrocyte and microglia

Astrocytes and microglia are the cells principally involved in brain immunity. The

immunohistochemical results (Figure 4) showed that the amount of both astrocytes and microglia in the SNpc region were largely increased and activated by MPTP/p treatment. 20C (50, 100 mg/kg) and selegiline could obviously suppress this activation ($p < 0.01$ for astrocytes, $p < 0.05$ for microglia).

Regulation of 20C on MPTP-induced NF-κB signaling and the NLRP3 inflammasome pathway

We showed (Figure 5A, 5B, 5C, and 5D) that MPTP/p could significantly increase the protein content of TLR4 ($p < 0.01$) (Figure 5A, 5B), NF-κB ($p < 0.001$) (Figure 5A, 5C) and NLRP3 ($p < 0.01$) (Figure 5A, 5D). Given that the activation of NLRP3 can lead to the cleavage of pro-caspase-1 (45 KDa) into p20 and p10, we detected the protein content of pro-caspase-1 (45 KDa) (Figure 5A, 5E), p20 (Figure 5A, 5F), and p10 (Figure 5G) with Western blot analysis or immunohistochemistry, and the results showed that MPTP/p led to a significant increase of caspase-1 (p20) and caspase-1 (p10). Activated caspase-1 can further shear and activate pro-IL-1β (35 KDa) and GSDMD. For IL-1β, the Western blot results showed that MPTP/p could apparently increase IL-1β content ($p < 0.05$ for 35 KDa, $p < 0.01$ for 15 KDa) (Figure 5H, 5I, and 5J), and the results of the immunohistochemistry described the same trend (Figure 5K). Inflammation is often accompanied by oxidative stress and we found the model SN region experienced serious oxidative stress damage as evident by heavily increased 8-hydroxyguanosine staining (Figure 5M). GSDMD (55 KDa) is a key protein mediating inflammatory death after shearing, and the laser scanning confocal results showed it was present in the dopaminergic neurons (Figure 5L). The results of the Western blot

analysis showed that the protein content of 55KDa-GSDMD was significant decreased ($p < 0.01$) after MPTP/p treatment (Figure 5N), which implied the activation of GSDMD. 20C and selegiline had a regulatory effect on these changes.

Discussion

In this study, we found that 20C played a protective role on the nigrostriatal system by reducing α-synuclein dysfunction and regulating α-synuclein related inflammatory responses, including BBB damage, glial activation, NF-κB signaling, and the NLRP3 inflammasome pathway (Figure 6).

α-Synuclein, a key factor for PD's degeneration, is highly expressed throughout the brain as a cytoplasmic protein with physiological functions such as regulating synaptic vesicles, altering synaptic plasticity, and serving as a molecular chaperone (Zhang et al., 2017b). However, abnormal α-synuclein is implicated in numerous degenerative diseases, including PD (Allen Reish and Standaert, 2015). Many studies have provided evidence that α-synuclein could exacerbate neuronal death as it inhibits tubulin polymerization (Chen et al., 2007), interacts with membranes (Pacheco et al., 2015), and augments oxidative stress(Gao et al., 2008). Moreover, aggregated α-synuclein could activate the inflammatory response by triggering the inflammasome and producing radicals (Gao et al., 2008; Codolo et al., 2013). In addition, modifications of α-synuclein, especially nitrative α-synuclein, could also potentiate the degeneration of neurons (Gao et al., 2008). The toxicity of nitrated α-synuclein involves (Gao et al., 2008; Schildknecht et al., 2013) the following: inhibiting both its own degradation and that of other proteins, decreasing α-synuclein binding to membranes, stabilizing the

monomer and inhibiting its fibrillization, and decreasing the clearance of α-synuclein. Whether the phosphorylation at Ser129 of α-synuclein is toxic remains unclear, but it is highly associated with PD because, among the total α-synuclein deposited in LBs, approximately 90% is phosphorylated at Ser129, whereas only 4% or less is phosphorylated in normal brains (Xu et al., 2015). The levels of Ser129-phosphorylated α-synuclein differ between patients with PD and healthy individuals in both blood plasma and the cerebrospinal fluid indicating its role as a useful biomarker for PD (Wang et al., 2012). Furthermore, the prion-like behavior of α-synuclein is closely associated to the progression of PD (Sacino et al., 2013). All in all, α-synuclein is a promising target for developing therapeutic strategies against neurodegenerative diseases. In our study, MPTP/p led to an increase of α-synuclein as well as its aggregation, nitration, and phosphorylation, and 20C administration could reduce the levels of α-synuclein and suppress its aggregation and nitration. 20C was unable to decrease phosphorylated α-synuclein levels; therefore its action is unrelated to the phosphorylation of α-synuclein.

Another key factor for PD's degeneration is neuroinflammation, which is closely with BBB permeation and glial activation. The brain had been ever taken as immune privileged because of its intact BBB structure, until peripheral immune cells were detected in the brain (Chen and Palmer, 2008; Brochard et al., 2009). Furthermore, the brain has its own resident immune cells, microglia, which comprise 20% of glial cells in the CNS and survey the brain for injuries (Chen and Palmer, 2008; Maguire-Zeiss and Federoff, 2010). Both the BBB and microglia have key roles in the development

and progression of neuroinflammation, which is involved in the degeneration observed in PD (Chen and Palmer, 2008; Chung et al., 2016). BBB damage would lead to the recruitment of T lymphocytes to the CNS and cause an inflammatory response by inducing microglial activation (Chen and Palmer, 2008; Chung et al., 2016), increasing the production of inflammatory factors, such as tumor necrosis factor alpha (TNF-α) and IL-1β. These toxicity mediators would in turn aggravate BBB damage (Reale et al., 2009). In addition to BBB and microglial cells, astrocytes are also widely accepted as pathological hallmarks in progressive diseases. On one hand, similar to microglia, astrocytes can trigger the release of pro-inflammatory factors (Halliday and Stevens, 2011); on the other hand, astrocytes can induce microglial activation to further accelerate the progress of neuroinflammation (Fellner et al., 2011; Halliday and Stevens, 2011; Barbierato et al., 2013; Facci et al., 2014). Both BBB leakage and glial activation have been discovered in clinical and in *in vivo* studies (Reale et al., 2009; Halliday and Stevens, 2011; Chung et al., 2016). In this study, we found BBB injury with severe swelling of astrocytic endfeet, largely activated microglia that became more amoeboidic by losing their ramifications, and activated astrocytes with enlarged bodies. 20C exhibited a protective effect against these abnormal alterations.

Actually, the two factors for PD's degeneration, α-synuclein dysfunction and neuroinflammation, can aggravate each other' toxicity by form a deteriorative cycle. Pathological α-synuclein can induce neuroinflammation and oxidative stress by glial activation and neuroinflammation can further cause the aggregation, nitration, and phosphorylation of α-synuclein. Moreover, α-synuclein can enhance the BBB

permeability (Jangula and Murphy, 2013) which can induce innate immunity and inflammation in brain. 20C may disrupt the vicious circle and prevent the progress of PD by targeting α-synuclein (Figure 6A).

The molecular mechanisms of neuroinflammation mainly involve NF-κB signaling and inflammasome pathway (Figure 6B) (Afonina et al., 2017). NF-κB signaling can be induced by α-synuclein through triggering the pattern recognition receptor TLR4 (Zhang et al., 2017b). After NF-κB activation, the inflammatory factors such as IL-1β will be largely produced (Zhang et al., 2017b). As for inflammasome, its formation requires a cytosolic pattern recognition receptor (PRR) as a sensor including NLRP1, NLRP3, NLRP6, NLRP7, NLRP12, NLRP4, and AIM2 (de Rivero Vaccari et al., 2014). Among these inflammasomes, NLRP3 inflammasome has been the most investigated one (de Rivero Vaccari et al., 2014). NLRP3 can be primed by TLR ligands and then trigger downstream caspae-1 signals(He et al., 2016). The activated caspase-1 is responsible for both maturation of IL-1β from pro-IL-1β and release of GSDMD N-terminus (GSDMD-NT) from GSDMD (Aglietti and Dueber, 2017). The mature IL-1β has a neurotoxic effect on the CNS, while the released GSDMD-NT can form pores on cell membrane by binding lipids to drive cell pyroptosis (Aglietti and Dueber, 2017). Further, pore formation in pyroptosis can accelerate the release of IL-1β from dying cells (Wright and Bryant, 2016), and activated IL-1β can promote the expression of NLRP3, which would in turn accelerate inflammasome pathway (He et al., 2016). In this study, MPTP/p treatment led to increase of TLR4, NF-κB, NLRP3, caspase-1, and IL-1β, and the decrease of GSDMD (55 KDa); therefore, α-synuclein-related NF-κB

JPET Fast Forward. Published on September 14, 2017 as DOI: 10.1124/jpet.117.244020
This article has not been copyedited and formatted. The final version may differ from this version.

signaling and NLRP3 inflammasome pathway activation may be involved in neuronal loss after MPTP/p treatment. 20C could regulate all these molecular changes.

In this study, we demonstrated the efficacy of 20C *in vivo* and proposed that 20C played its protective role by reducing pathological α-synuclein and suppressing neuroinflammation. Further, at the level of molecular mechanisms, 20C could inhibit the activation of the NF-κB and NLRP3 inflammasome pathway, reducing both IL-1β release and inflammatory cell death (pyroptosis).

Acknowledgments

The authors thank Zheng Mu, Peng-Fei Yang, Jv-Yang Huang and Cong-Yuan Xia for providing technical assistance.

Authorship Contributions

Participated in research design: Yu-He Yuan, Nai-hong Chen, and Qiu-Shuang Zhang

Conducted experiments: Qiu-Shuang Zhang, Yang Heng, Ying Chen, Piao Luo, Lu Wen, and Zhao Zhang

Performed data analysis: Qiu-Shuang Zhang

Wrote or contributed to writing of the manuscript: Qiu-Shuang Zhang

References

Afonina IS, Zhong Z, Karin M and Beyaert R (2017) Limiting inflammation-the negative regulation of NF-kappaB and the NLRP3 inflammasome. **18**:861-869.

Aglietti RA and Dueber EC (2017) Recent Insights into the Molecular Mechanisms Underlying Pyroptosis and Gasdermin Family Functions. *Trends in immunology* **38**:261-271.

Allen Reish HE and Standaert DG (2015) Role of alpha-synuclein in inducing innate and adaptive immunity in Parkinson disease. *Journal of Parkinson's disease* **5**:1-19.

Barbierato M, Facci L, Argentini C, Marinelli C, Skaper SD and Giusti P (2013) Astrocyte-microglia cooperation in the expression of a pro-inflammatory phenotype. *CNS & neurological disorders drug targets* **12**:608-618.

Bove J and Perier C (2012) Neurotoxin-based models of Parkinson's disease. *Neuroscience* **211**:51-76.

Brochard V, Combadiere B, Prigent A, Laouar Y, Perrin A, Beray-Berthat V, Bonduelle O, Alvarez-Fischer D, Callebert J, Launay JM, Duyckaerts C, Flavell RA, Hirsch EC and Hunot S (2009) Infiltration of CD4+ lymphocytes into the brain contributes to neurodegeneration in a mouse model of Parkinson disease. *The Journal of clinical investigation* **119**:182-192.

Chen L, Jin J, Davis J, Zhou Y, Wang Y, Liu J, Lockhart PJ and Zhang J (2007) Oligomeric alpha-synuclein inhibits tubulin polymerization. *Biochemical and biophysical research communications* **356**:548-553.

Chen Z and Palmer TD (2008) Cellular repair of CNS disorders: an immunological perspective. *Human molecular genetics* **17**:R84-92.

Chung YC, Shin WH, Baek JY, Cho EJ, Baik HH, Kim SR, Won SY and Jin BK (2016) CB2 receptor activation prevents glial-derived neurotoxic mediator production, BBB leakage and peripheral immune cell infiltration and rescues dopamine neurons in the MPTP model of Parkinson's disease. *Experimental & molecular medicine* **48**:e205.

Codolo G, Plotegher N, Pozzobon T, Brucale M, Tessari I, Bubacco L and de Bernard M (2013) Triggering of inflammasome by aggregated alpha-synuclein, an inflammatory response in synucleinopathies. *PloS one* **8**:e55375.

Connolly BS and Lang AE (2014) Pharmacological treatment of Parkinson disease: a review. *Jama* **311**:1670-1683.

Dauer W and Przedborski S (2003) Parkinson's disease: mechanisms and models. *Neuron* **39**:889-909.

de Rivero Vaccari JP, Dietrich WD and Keane RW (2014) Activation and regulation of cellular inflammasomes: gaps in our knowledge for central nervous system injury. *Journal of cerebral blood flow and metabolism : official journal of the International Society of Cerebral Blood Flow and Metabolism* **34**:369-375.

Facci L, Barbierato M, Marinelli C, Argentini C, Skaper SD and Giusti P (2014) Toll-like receptors 2, -3 and -4 prime microglia but not astrocytes across central nervous system regions for ATP-dependent interleukin-1beta release. *Scientific reports* **4**:6824.

Fellner L, Jellinger KA, Wenning GK and Stefanova N (2011) Glial dysfunction in the pathogenesis of alpha-synucleinopathies: emerging concepts. *Acta neuropathologica* **121**:675-693.

Gao HM, Kotzbauer PT, Uryu K, Leight S, Trojanowski JQ and Lee VM (2008) Neuroinflammation and oxidation/nitration of alpha-synuclein linked to dopaminergic neurodegeneration. *The Journal of neuroscience : the official journal of the Society for Neuroscience* **28**:7687-7698.

Halliday GM and Stevens CH (2011) Glia: initiators and progressors of pathology in Parkinson's disease.

Movement disorders : official journal of the Movement Disorder Society **26**:6-17.

He Y, Hara H and Nunez G (2016) Mechanism and Regulation of NLRP3 Inflammasome Activation. *Trends in biochemical sciences* **41**:1012-1021.

Heng Y, Zhang QS, Mu Z, Hu JF, Yuan YH and Chen NH (2016) Ginsenoside Rg1 attenuates motor impairment and neuroinflammation in the MPTP-probenecid-induced parkinsonism mouse model by targeting alpha-synuclein abnormalities in the substantia nigra. *Toxicology letters* **243**:7-21.

Huang JY, Yuan YH, Yan JQ, Wang YN, Chu SF, Zhu CG, Guo QL, Shi JG and Chen NH (2016) 20C, a bibenzyl compound isolated from Gastrodia elata, protects PC12 cells against rotenone-induced apoptosis via activation of the Nrf2/ARE/HO-1 signaling pathway. *Acta pharmacologica Sinica* **37**:731-740.

Jangula A and Murphy EJ (2013) Lipopolysaccharide-induced blood brain barrier permeability is enhanced by alpha-synuclein expression. *Neuroscience letters* **551**:23-27.

Liu LF, Song JX, Lu JH, Huang YY, Zeng Y, Chen LL, Durairajan SS, Han QB and Li M (2015) Tianma Gouteng Yin, a Traditional Chinese Medicine decoction, exerts neuroprotective effects in animal and cellular models of Parkinson's disease. *Scientific reports* **5**:16862.

Maguire-Zeiss KA and Federoff HJ (2010) Future directions for immune modulation in neurodegenerative disorders: focus on Parkinson's disease. *Journal of neural transmission (Vienna, Austria : 1996)* **117**:1019-1025.

Mou Z, Yuan YH, Lou YX, Heng Y, Huang JY, Xia CY, Gao Y, Zhu CG, Chu SF, Luo P, Shi JG and Chen NH (2016) Bibenzyl compound 20c protects against endoplasmic reticulum stress in tunicamycin-treated PC12 cells in vitro. *Acta pharmacologica Sinica* **37**:1525-1533.

Ojemann LM, Nelson WL, Shin DS, Rowe AO and Buchanan RA (2006) Tian ma, an ancient Chinese herb, offers new options for the treatment of epilepsy and other conditions. *Epilepsy & behavior : E&B* **8**:376-383.

Pacheco CR, Morales CN, Ramirez AE, Munoz FJ, Gallegos SS, Caviedes PA, Aguayo LG and Opazo CM (2015) Extracellular alpha-synuclein alters synaptic transmission in brain neurons by perforating the neuronal plasma membrane. *Journal of neurochemistry* **132**:731-741.

Reale M, Iarlori C, Thomas A, Gambi D, Perfetti B, Di Nicola M and Onofrj M (2009) Peripheral cytokines profile in Parkinson's disease. *Brain, behavior, and immunity* **23**:55-63.

Sacino AN, Brooks M, McGarvey NH, McKinney AB, Thomas MA, Levites Y, Ran Y, Golde TE and Giasson BI (2013) Induction of CNS alpha-synuclein pathology by fibrillar and non-amyloidogenic recombinant alpha-synuclein. *Acta neuropathologica communications* **1**:38.

Schildknecht S, Gerding HR, Karreman C, Drescher M, Lashuel HA, Outeiro TF, Di Monte DA and Leist M (2013) Oxidative and nitrative alpha-synuclein modifications and proteostatic stress: implications for disease mechanisms and interventions in synucleinopathies. *Journal of neurochemistry* **125**:491-511.

Wang Y, Shi M, Chung KA, Zabetian CP, Leverenz JB, Berg D, Srulijes K, Trojanowski JQ, Lee VM, Siderowf AD, Hurtig H, Litvan I, Schiess MC, Peskind ER, Masuda M, Hasegawa M, Lin X, Pan C, Galasko D, Goldstein DS, Jensen PH, Yang H, Cain KC and Zhang J (2012) Phosphorylated alpha-synuclein in Parkinson's disease. *Science translational medicine* **4**:121ra120.

Wright JA and Bryant CE (2016) The killer protein Gasdermin D. *Cell death and differentiation* **23**:1897-1898.

Xu Y, Deng Y and Qing H (2015) The phosphorylation of alpha-synuclein: development and implication

for the mechanism and therapy of the Parkinson's disease. *Journal of neurochemistry* **135**:4-18.

Zhang QS, Heng Y, Mou Z, Huang JY, Yuan YH and Chen NH (2017a) Reassessment of subacute MPTP-treated mice as animal model of Parkinson's disease. *Acta pharmacologica Sinica*.

Zhang QS, Heng Y, Yuan YH and Chen NH (2017b) Pathological alpha-synuclein exacerbates the progression of Parkinson's disease through microglial activation. *Toxicology letters* **265**:30-37.

Zhang XL, Yuan YH, Shao QH, Wang ZZ, Zhu CG, Shi JG, Ma KL, Yan X and Chen NH (2017c) DJ-1 regulating PI3K-Nrf2 signaling plays a significant role in bibenzyl compound 20C-mediated neuroprotection against rotenone-induced oxidative insult. *Toxicology letters* **271**:74-83.

Footnote

This work was supported by the National Natural Science Foundation of China Grants [81773925, U1402221, 81573640, 81603316], Beijing Natural Science Foundation [NO.7161011], CAMS Innovation Fund for Medical Sciences (CIFMS) [2016-I2M-1-004], Key Research and Development Project of Hunan Province [2015SK2029-1], and the Scientific Research Foundation of the Higher Education Institutions of Hunan Province [15K091].

Figure Legends

Figure 1. Experimental procedure, body weight, and pole test. (A) Chemical structure of 20C. (B) Treatment for each group. (C) Schedule for this study. (D) There was no difference for body weight among groups. (E) 20C could improve motor impairment in the pole test. Data are presented as mean ± SEM, n > 10. One-way ANOVA followed by Duncan's post hoc tests. *** $p < 0.001$, $^{\#}$ $p < 0.05$, $^{\#\#\#}$ $p < 0.001$ *vs* the control group.

Figure 2. 20C had a protective effect on the nigrostriatal system. (A, B, C) 20C could attenuate DA depletion and DA turnover. (D, E, F, G, H) 20C could reduce the loss of dopaminergic cells in the substantia nigra pars compacta (SNpc) and terminals in the striatum. (D, E) Immunohistochemical staining of tyrosine hydroxylase (TH) in the nigrostriatal system. (F) Western blot result of TH protein level in the striatum. (G, H) Quantitative analysis of TH^+ cells in the SNpc and striatum. (I, J, K) 20C could ameliorate ultrastructure destruction in the SNpc region. As indicated by the red arrows, the model neuron is severely damaged with heavy electron density (I) and swollen organelles (J), and the structure of the blood brain barrier (BBB) is seriously destroyed (K), which could be improved by 20C and selegiline. Data are presented as mean ± SEM, n = 3. One-way ANOVA followed by Duncan's post hoc tests. * $p < 0.05$, *** $p < 0.001$ *vs* the control group; $^{\#}$ $p < 0.05$, $^{\#\#}$ $p < 0.01$, $^{\#\#\#}$ $p < 0.001$ *vs* the model group.

Figure 3. 20C could ameliorate 1-methyl-4-phenyl-1, 2, 3, 6-tetrahydropyridine/probenecid (MPTP/p) induced α-synuclein dysfunction. (A, B, C, D)

Western blot results of α-synuclein (C20), aggregated α-synuclein (5G4), nitrated Tyr125/Tyr133 α-synuclein, and phosphorylated Ser129 α-synuclein. (E, F) Immunohistochemical results of aggregated α-synuclein (5G4) and nitrated Tyr125/Tyr133 α-synuclein. Data are presented as mean ± SEM, n = 3. One-way ANOVA followed by Duncan's post hoc tests. *$p < 0.05$, **$p < 0.01$ *vs* the control group; $^{\#}p < 0.05$, $^{\#\#}p < 0.01$ *vs* the model group.

Figure 4. 20C could suppress the activation of microglia and astrocytes in the SNpc. (A, B) Immunohistochemical staining of Iba-1^{+} and GFAP^{+} cells. (C, D) Quantitative analysis of Iba-1^{+} and GFAP^{+} cells. Data are presented as mean ± SEM, n = 3. One-way ANOVA followed by Duncan's post hoc tests. ** $p < 0.01$, *** $p < 0.001$ *vs* the control group; $^{\#}$ $p < 0.05$, $^{\#\#}$ $p < 0.01$ *vs* the model group.

Figure 5. Regulation of 20C on MPTP-induced NF-κB signaling and the NLRP3 inflammasome pathway. (A) Western blot bands of TLR4, NF-κB, NLRP3, and caspase-1 (pro- and p20). (B, C, D, E, F) Western blot analysis of TLR4, NF-κB, NLRP3, and caspase-1 (pro- and p20). (G) Immunohistochemical result of caspase-1(p10). (H, I, J, K) Western blot and immunohistochemical results of IL-1β. (M) Immunohistochemical result of 8-hydroxyguanosine. (L) Laser scanning confocal result of GSDMD and TH. (N) Western blot result of 55KDa-GSDMD. Data are presented as mean ± SEM, n = 3. One-way ANOVA followed by Duncan's post hoc tests. *$p < 0.05$, **$p < 0.01$, ***$p < 0.001$ *vs* the control group; $^{\#}p < 0.05$, $^{\#\#}p < 0.01$ *vs*

the model group.

Figure 6. Summary for this research. (A) 20C could prevent progressive neurodegeneration by interrupting the deteriorative cycle formed by BBB damage, glial activation, and α-synuclein abnormality. (B) 20C could inhibit the activation of the NF-κB pathway and NLRP3 inflammasome, reducing both IL-1β release and inflammatory cell death (pyroptosis).

JPET Fast Forward. Published on September 14, 2017 as DOI: 10.1124/jpet.117.244020
This article has not been copyedited and formatted. The final version may differ from this version.

Figures

Figure 1

A

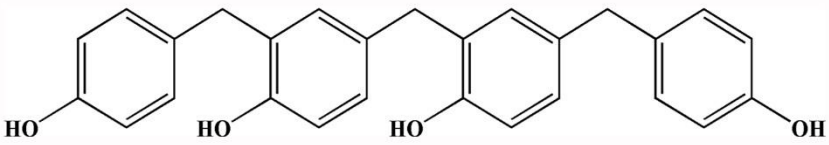

B

Groups	Ctrl	Model	20C			Sele
p.o.	CMCNa	CMCNa	20C(25mg/kg	50mg/kg	100mg/kg)	selegiline(3mg/kg)
i.p.	probenecid	probenecid	probenecid	probenecid	probenecid	probenecid
s.c.	NS	MPTP	MPTP	MPTP	MPTP	MPTP

C

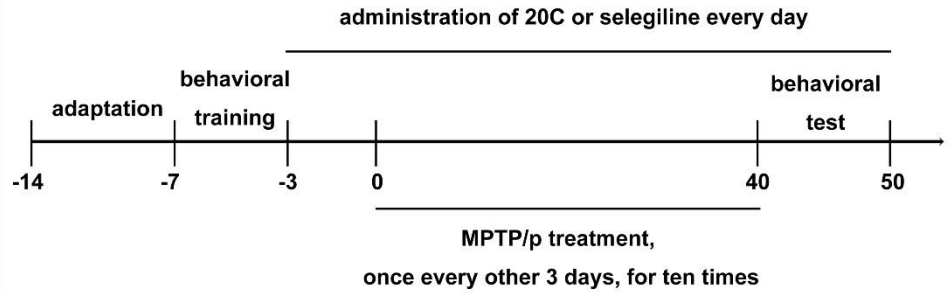

D

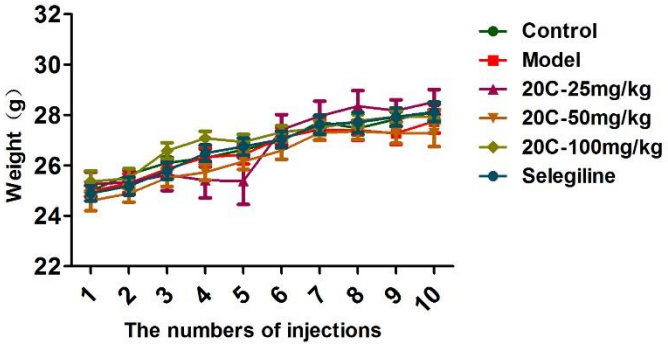

E

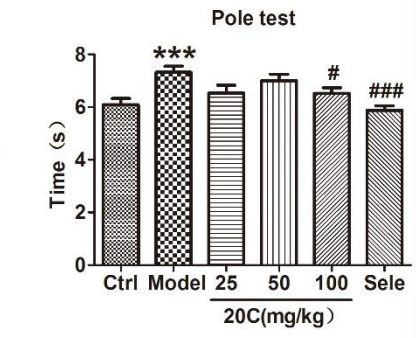

JPET Fast Forward. Published on September 14, 2017 as DOI: 10.1124/jpet.117.244020
This article has not been copyedited and formatted. The final version may differ from this version.

Figure 2

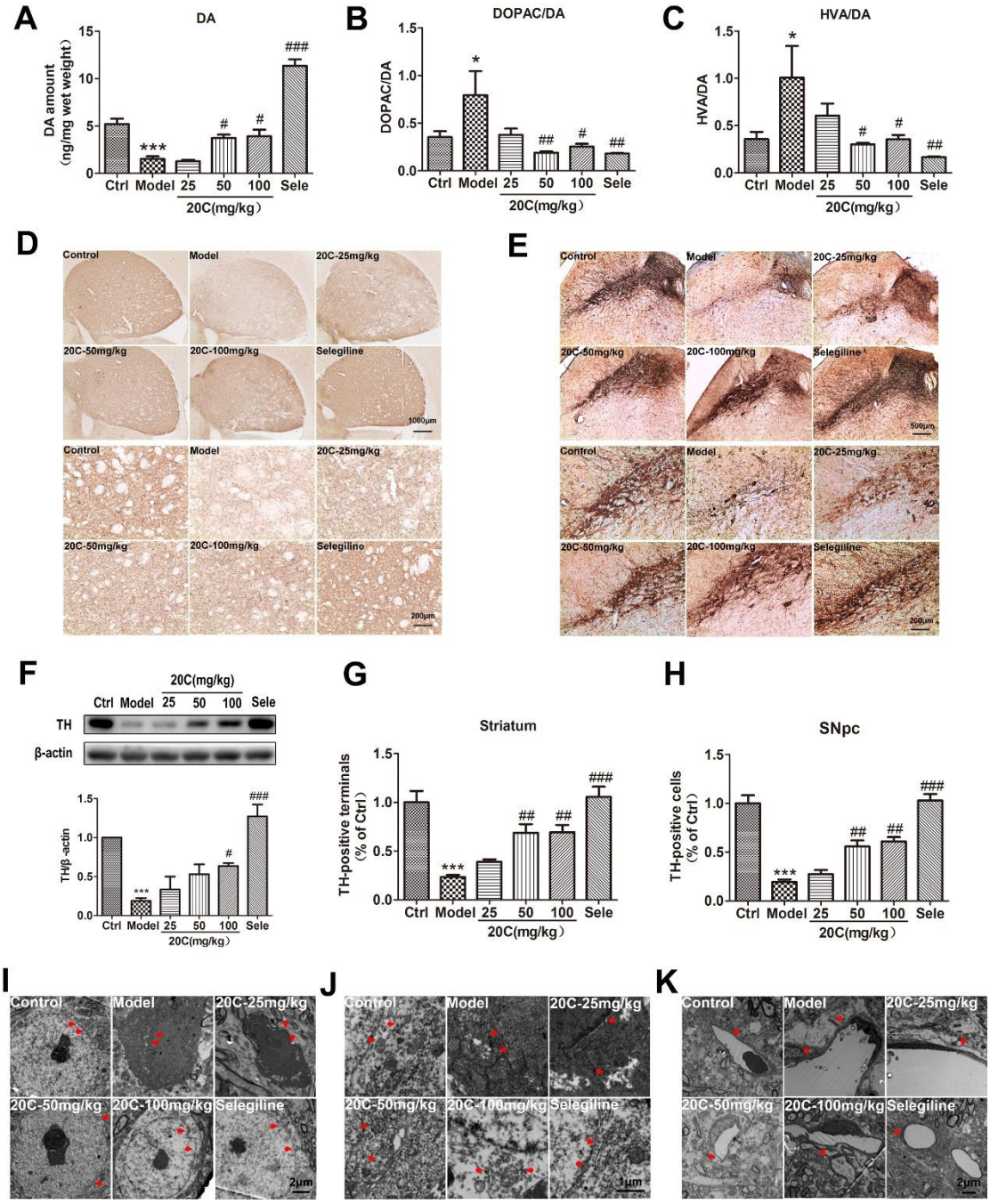

JPET Fast Forward. Published on September 14, 2017 as DOI: 10.1124/jpet.117.244020
This article has not been copyedited and formatted. The final version may differ from this version.

Figure 3

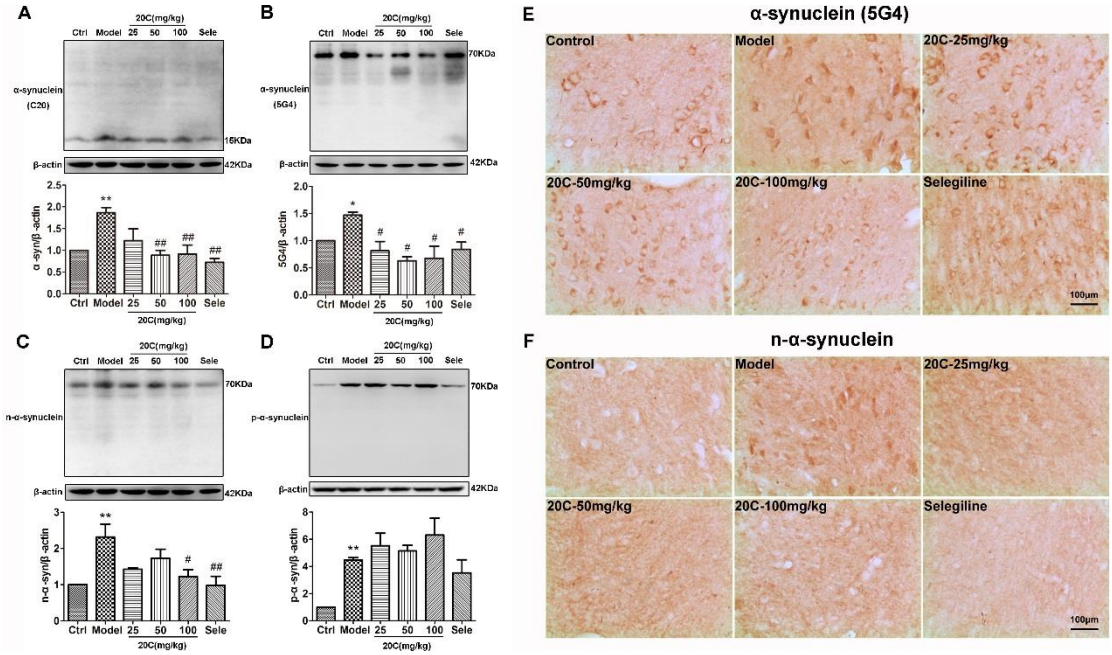

JPET Fast Forward. Published on September 14, 2017 as DOI: 10.1124/jpet.117.244020
This article has not been copyedited and formatted. The final version may differ from this version.

Figure 4

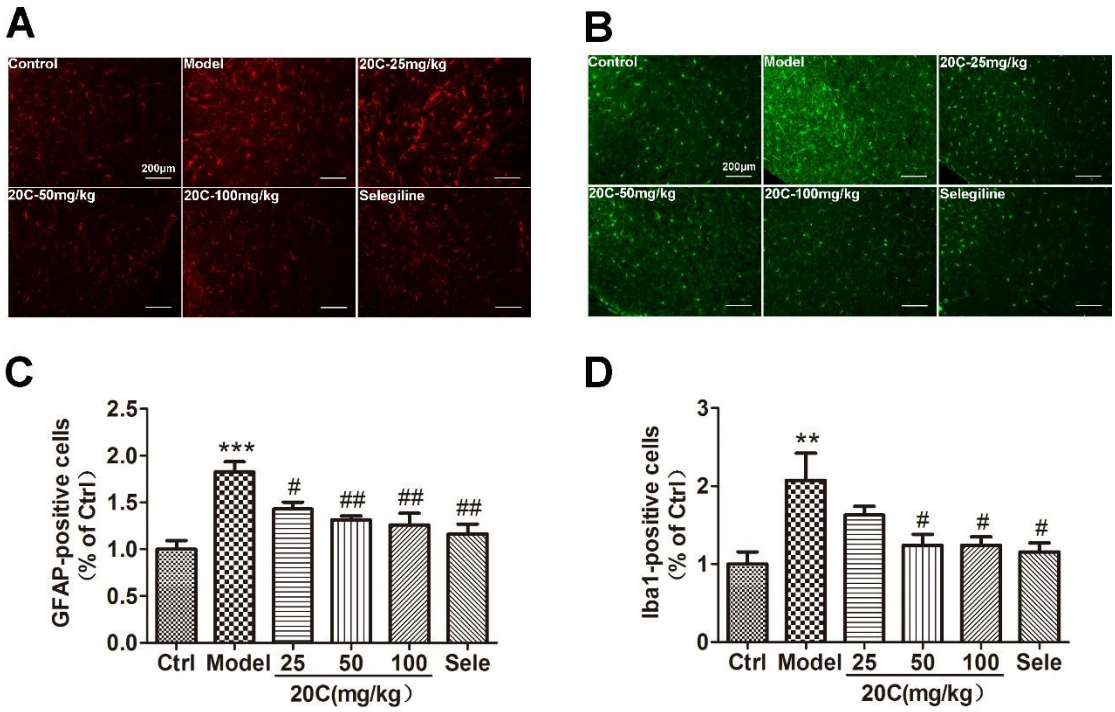

JPET Fast Forward. Published on September 14, 2017 as DOI: 10.1124/jpet.117.244020
This article has not been copyedited and formatted. The final version may differ from this version.

Figure 5

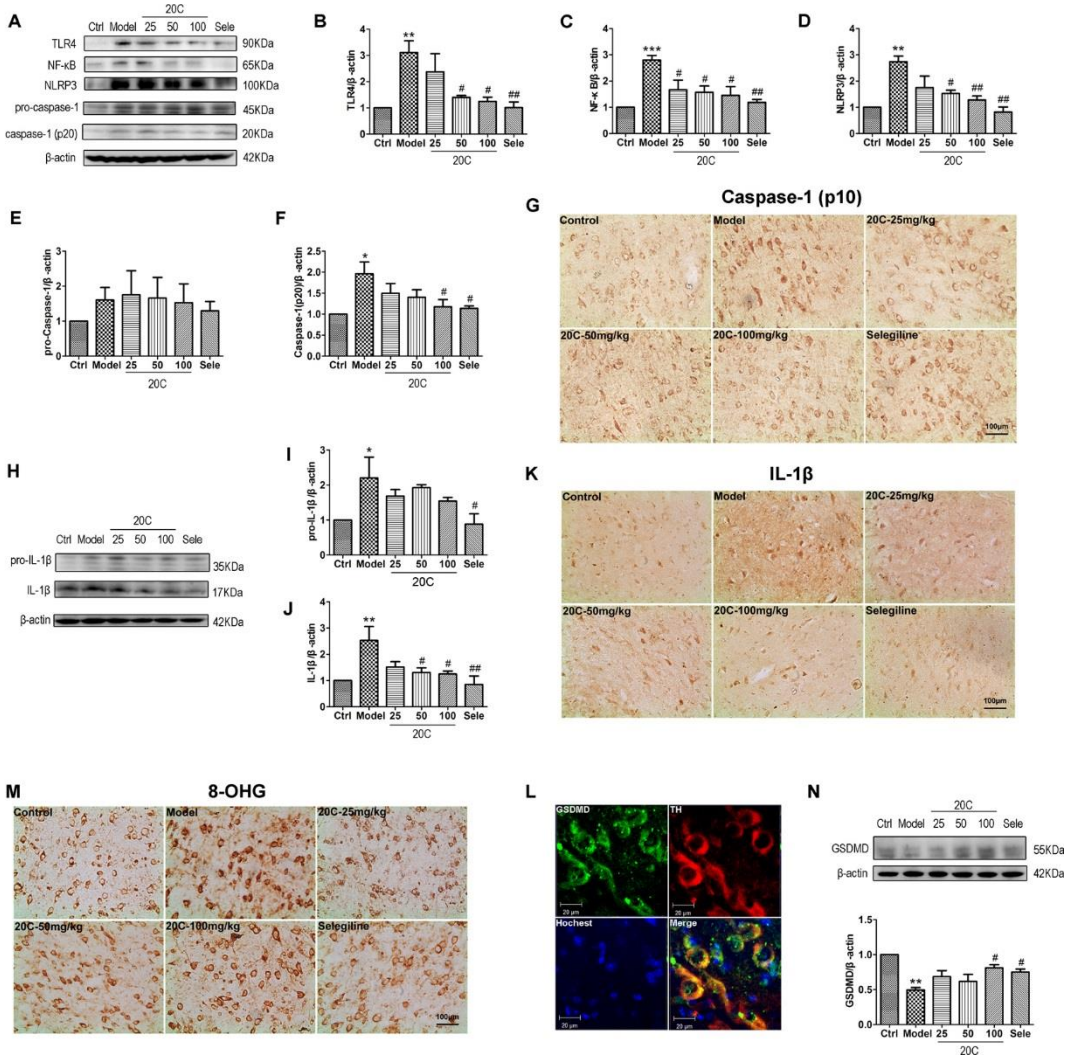

JPET Fast Forward. Published on September 14, 2017 as DOI: 10.1124/jpet.117.244020
This article has not been copyedited and formatted. The final version may differ from this version.

Figure 6